Radiation and particle acceleration processes in relativistic outflows

E.V. Derishev

Institute of Applied Physics
Nizhny Novgorod, Russia

XXVI Baikal International Summer School
on Physics of Elementary Particles and Astrophysics

Summary of Lecture 1

- Broadband non-thermal emission from relativistic outflows covers over 10 orders of magnitude in frequency.
- A typical broadband spectrum has two widely separated peaks:
  - lower-energy component is due to synchrotron emission
  - higher-energy component is due to inverse Compton emission
- Consistent formulation of the synchrotron-self-Compton model requires that QED effects are taken into account
- One-zone SSC model provides good spectral fits in many cases, yet it is not a master key that opens every door.

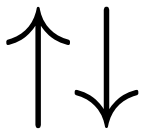
Lecture 2

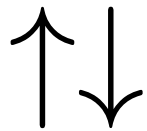
1. The conventional view of particle acceleration and its pitfalls
2. Pair balance: joining radiation and acceleration into a single model
3. Inferring the magnetic field properties from GRB afterglow observations
4. Insights from particle-in-cell simulations

Main building blocks of a full physical model

Radiation processes

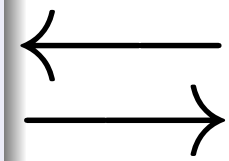
- Synchrotron radiation
- Inverse Compton with same electrons, interacting with soft photons including synchrotron
- ...





Particle acceleration

- Diffusive shock acceleration
- Shear flow acceleration
- Reconnection
- Converter acceleration
- ...



Magnetic field

- Frozen-in magnetic field
- Turbulent dynamo
- Weibel instability
- ...

Conventional view of acceleration as standalone process

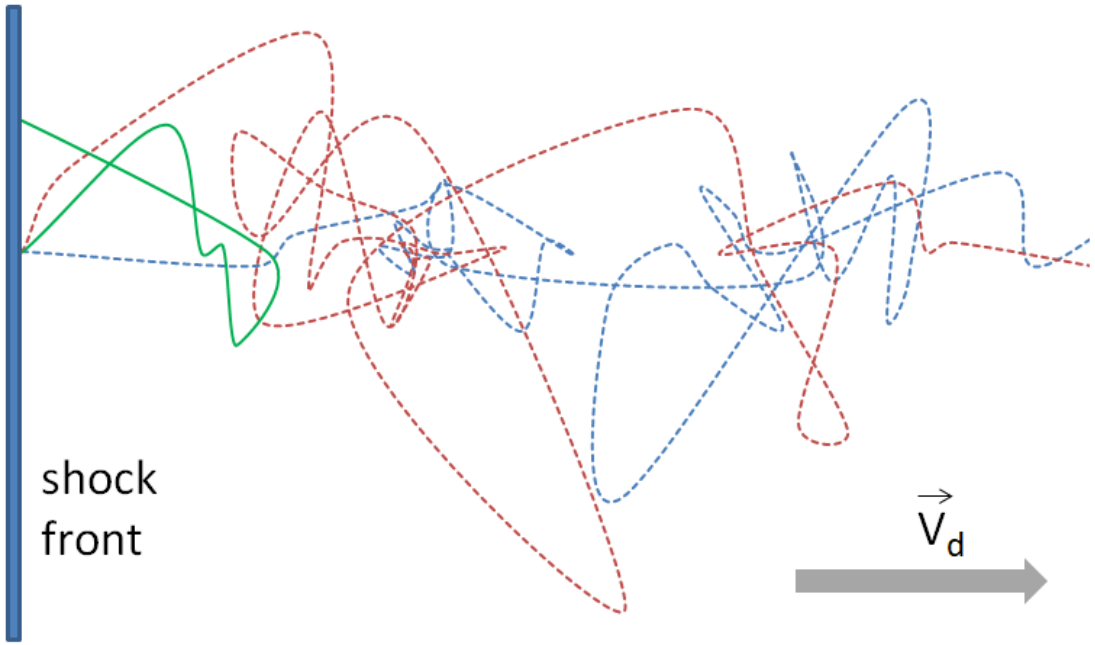
Diffusive shock acceleration

- Avg. Lorentz factor of injected electrons $\langle\gamma_{\rm inj}\rangle = (\epsilon_e/\xi_e)\Gamma_{\rm sh}(m_p/m_e)$.
- Fraction of energy in accelerated electrons $\epsilon_e \sim 0.1$, similar to what is seen in PIC simulations.
- Fraction of electrons being accelerated $\xi_e = 1$. PIC simulations show $\xi_e \sim 0.1$.

Acceleration in jets

- Many options: shocks, reconnection, shear acceleration ...
- Both $\xi_e \sim 0.1$ and ϵ_e are not universal constants
- $\langle\gamma_{\rm inj}\rangle = ?$ — assume whatever we think is realistic

Acceleration at relativistic shocks: analytics



Effective width of downstream "reflection layer" is $\simeq \dfrac{1-\beta_d}{\beta_d}$ mean free paths

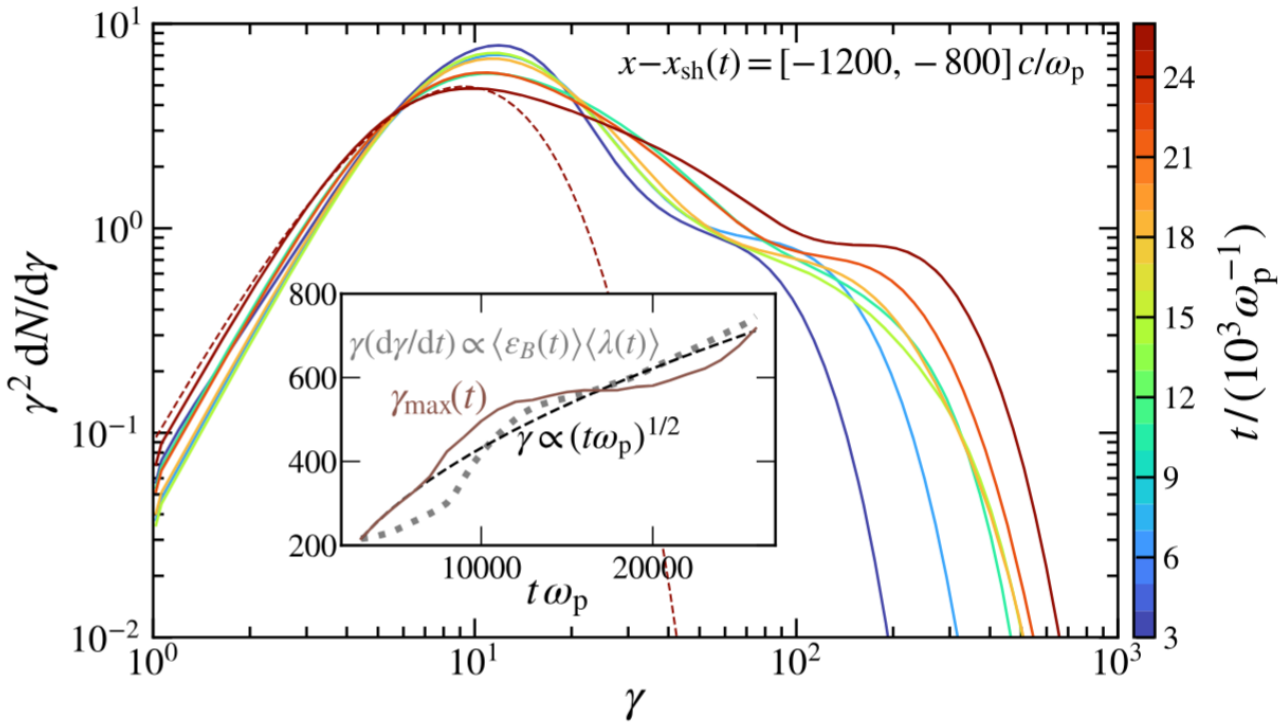
This is only $\simeq$ 2 m.f.p. in relativistic shocks ($\beta_d = 1/3$) — diffusion approximation is questionable

Expectations

- No Fermi acceleration with regular magnetic field
- Within diffusion approximation accelerated particles form a power-law distribution with $p = \dfrac{\beta_d^3 - 2\beta_d^2 + 2\beta_d + 1}{1-\beta_d}$, that is $p = \dfrac{20}{9} \simeq 2.22$

Keshet & Waxman 2005

Acceleration at relativistic shocks: longest simulations

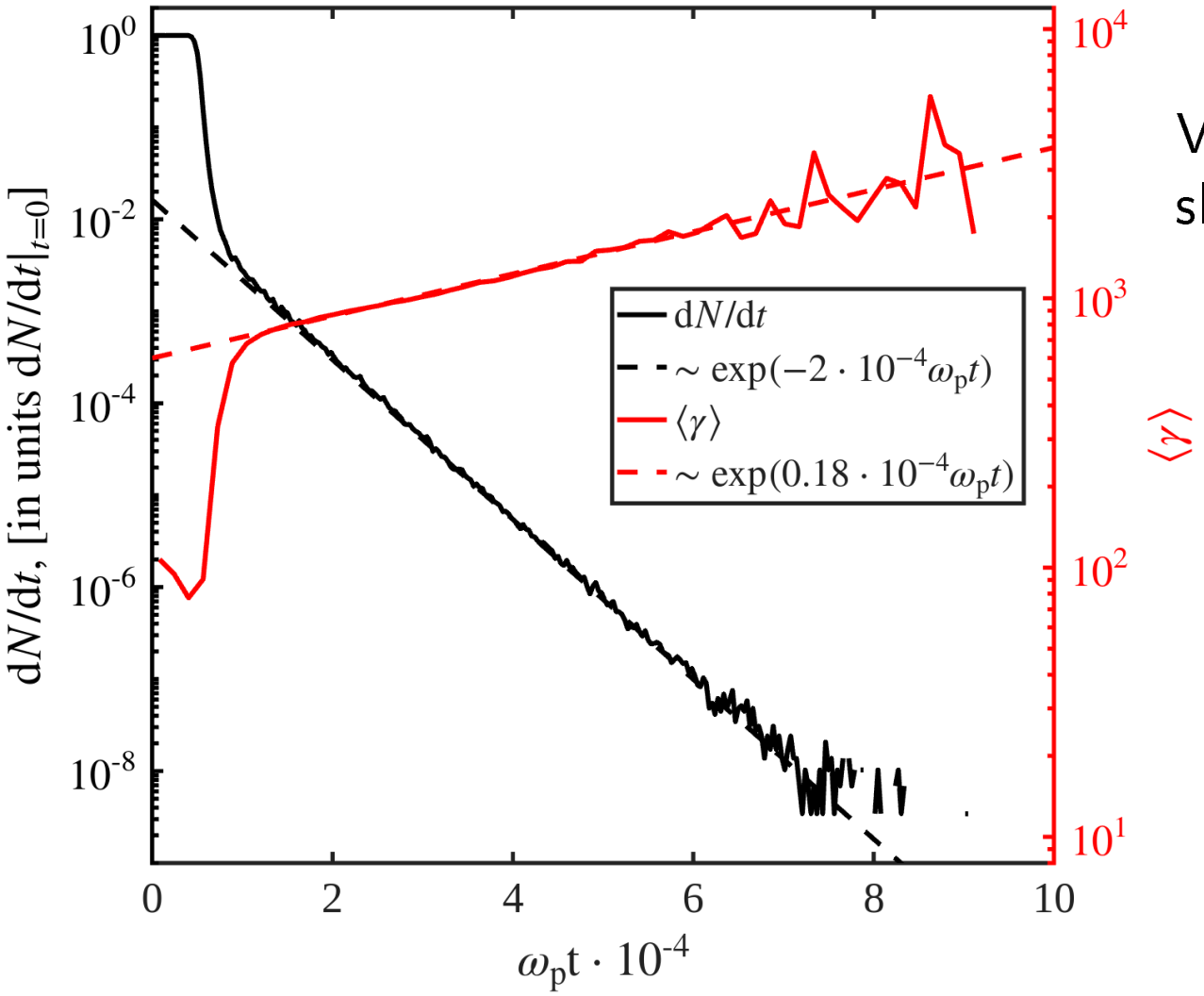


Even the longest runs don't reach steady state

Grošelj, Sironi & Spitkovsky
ApJ 963 (2024)

- fraction of energy in accelerated electrons $\epsilon_e \sim 0.1$
- magnetization near the front $\epsilon_{\rm B} \sim 0.01$
- magnetic field short-lived; persists somewhat longer in longer runs

Fermi acceleration: how close is the limit?

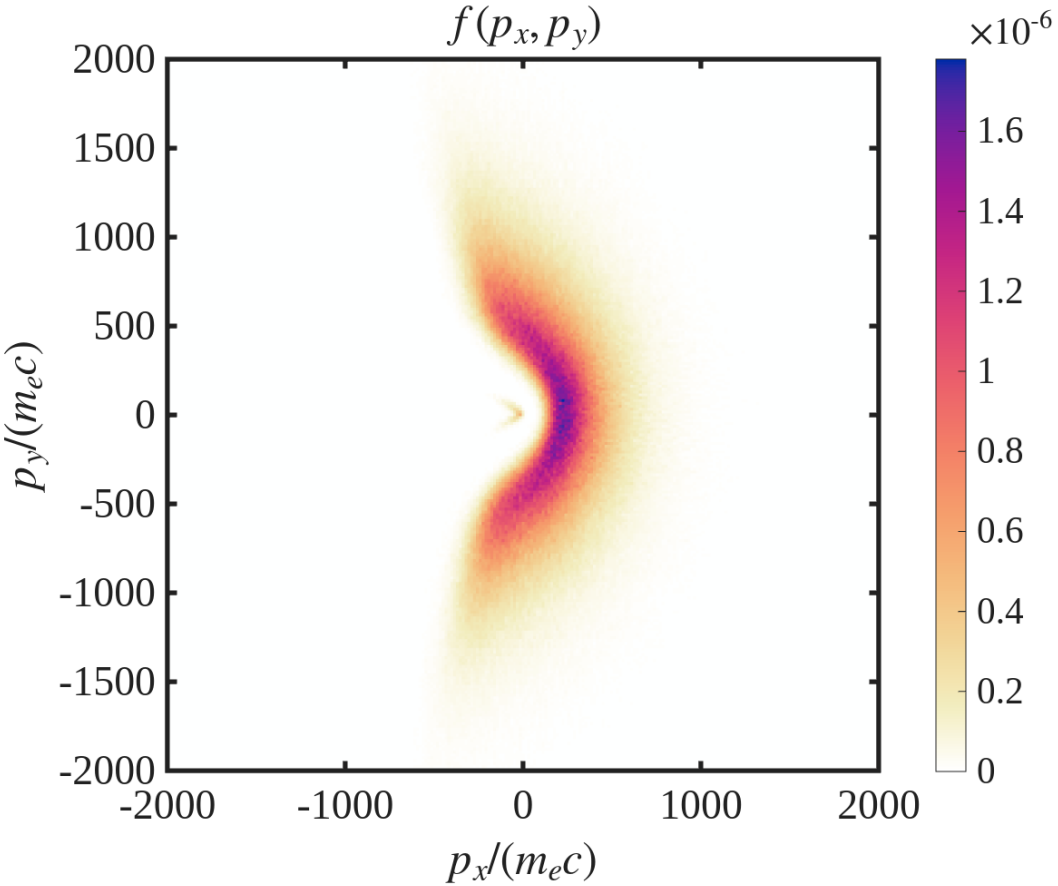


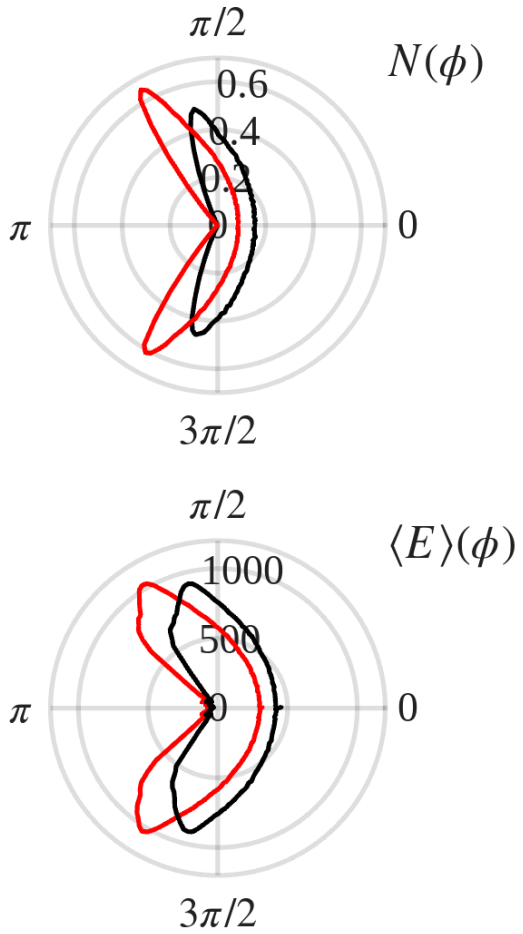
Very long simulation in the shock-comoving frame

Garasev & ED,
to appear on arXiv

Fast acceleration ceases after increasing particles' energy approx. 10-fold

Angular distribution of accelerated particles: evidence of low scattering limit





black – front-comoving frame

red – zero-momentum frame

Garasev & ED, to appear on arXiv

Second revision: SSC → pair-balance model

Question

What happens to secondary pairs
when they are created upstream of a highly relativistic shock?

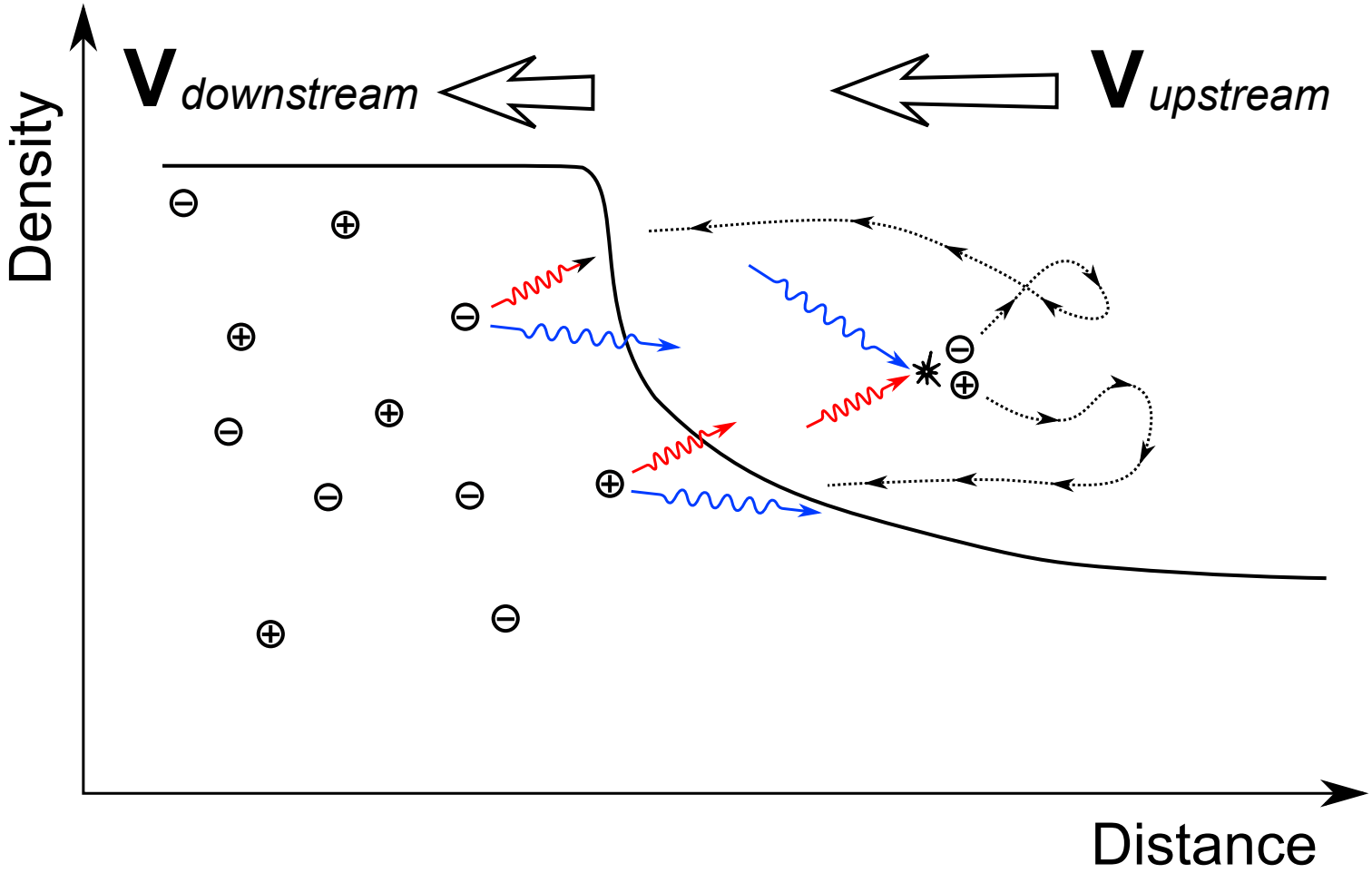
Answer

The converter acceleration mechanism switches on,
far outweighing the diffusive shock acceleration

- Is every GRB afterglow consistent with reduced 3D parameter space of the pair-balance model?
  so far – yes, but statistics is low
- Can pair-balance model facilitate generation of long-lived magnetic field?
- What is the exact shape of the primary injection function?

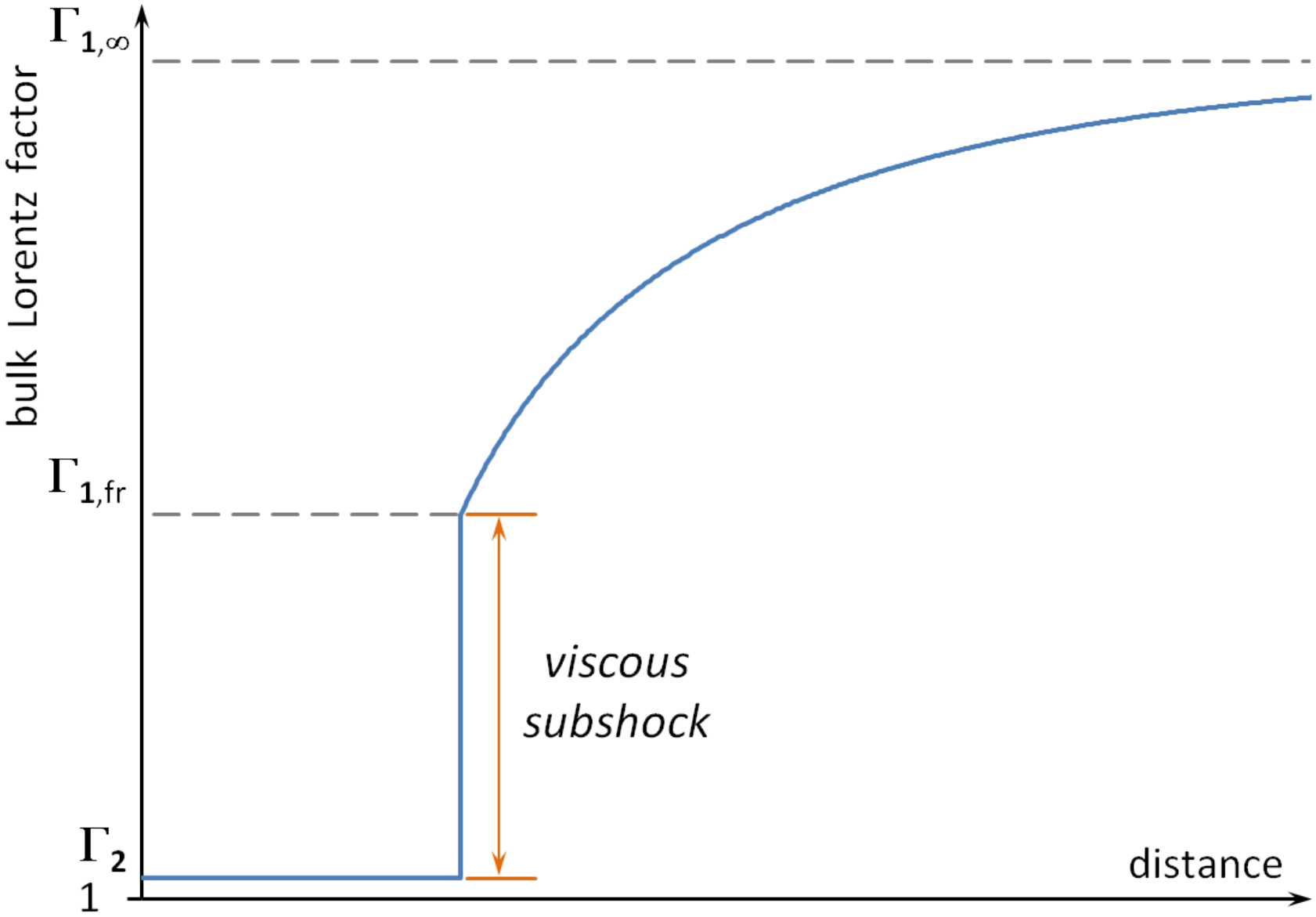
Pair-balance shock

Figure from Derishev and Piran, ApJ 923 (2021)

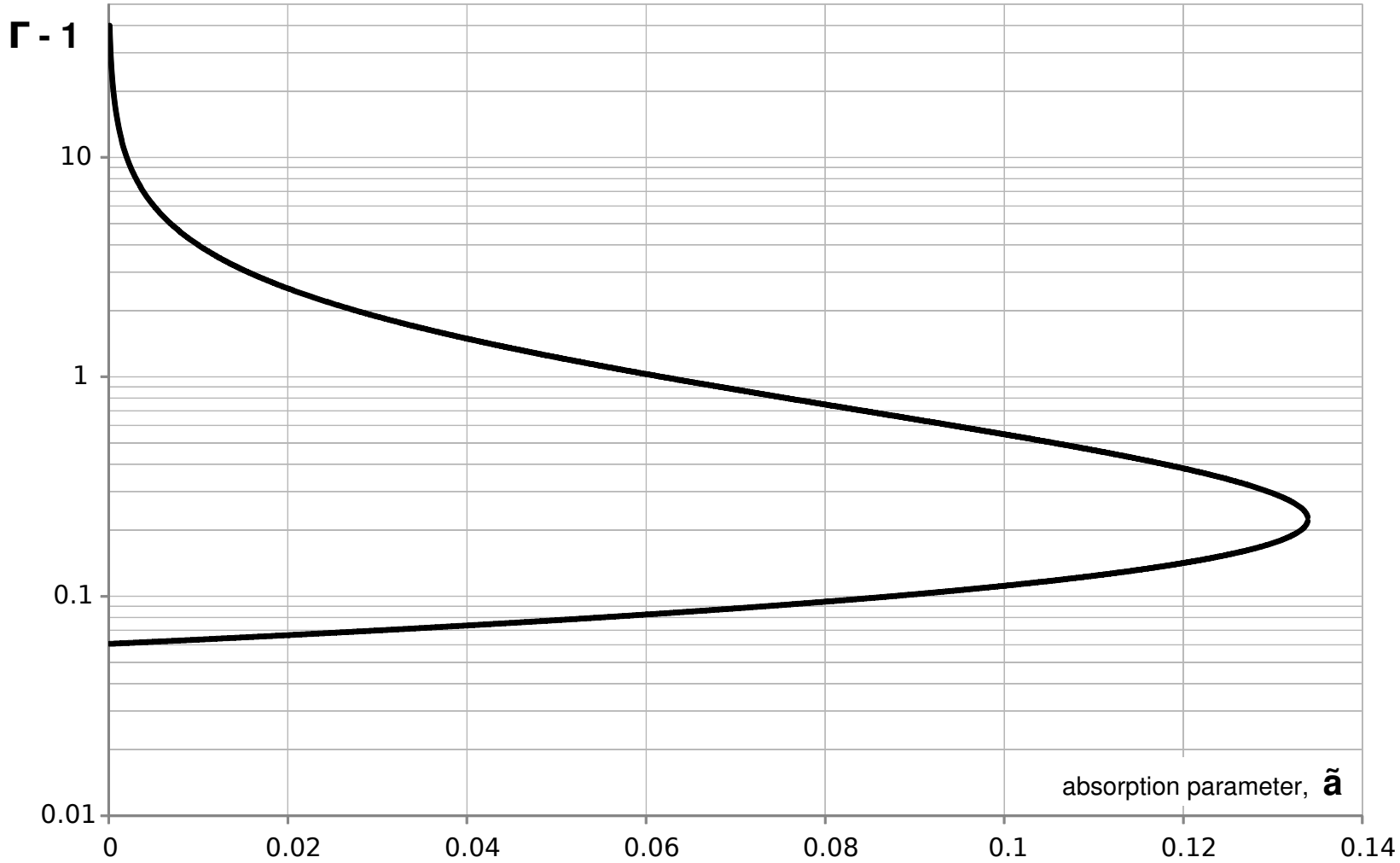


- efficient acceleration $\Rightarrow$ fraction of absorbed radiation rises
- absorbed fraction $\gtrsim 0.1$ makes acceleration inefficient

Structure of the modified relativistic shock



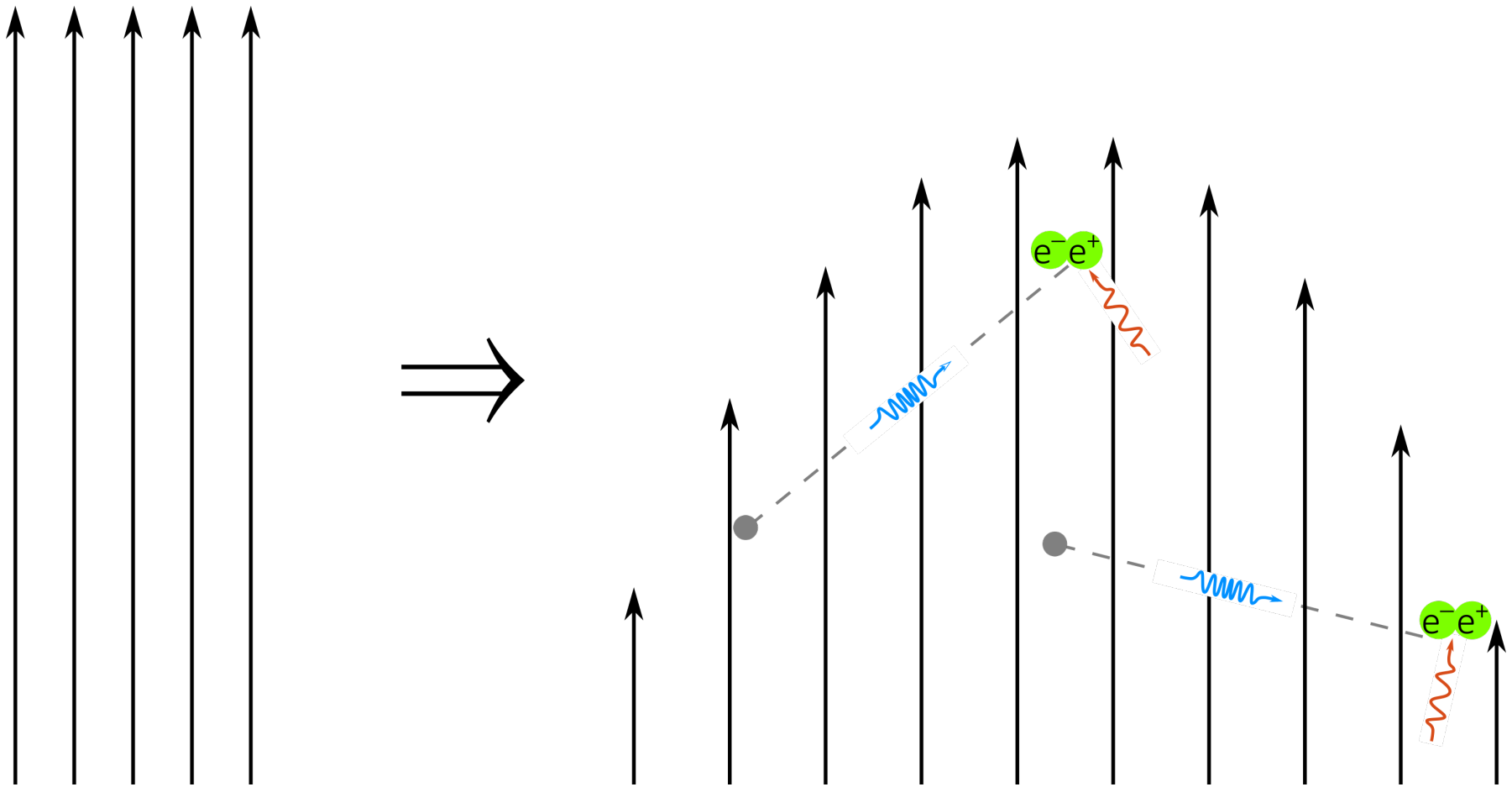
Velocities at viscous subshock



Bulk Lorentz factors in shock-front comoving frame

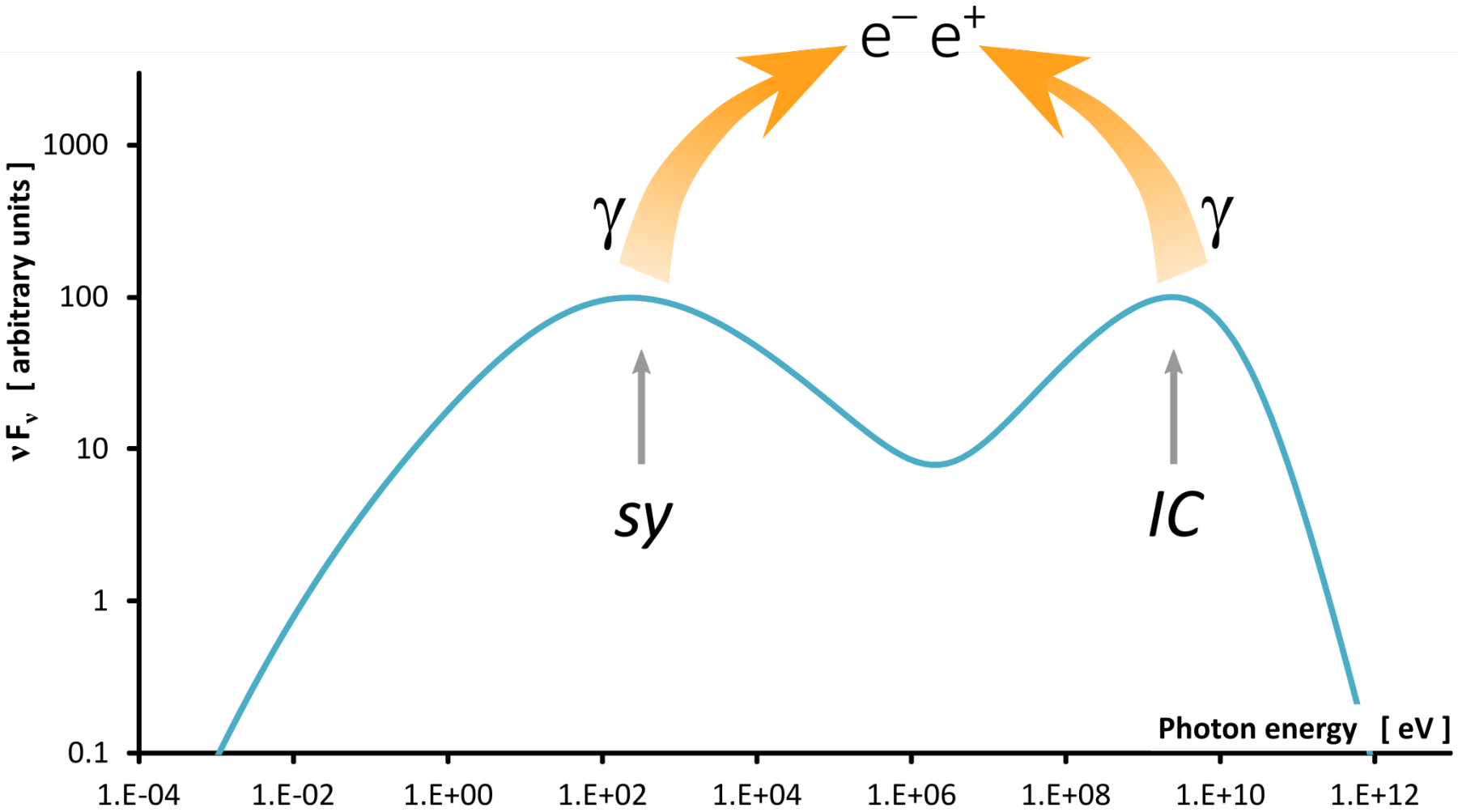
upper branch – the upstream
lower branch – the downstream.

Energy and momentum transfer by $e^- e^+$-pairs across jets



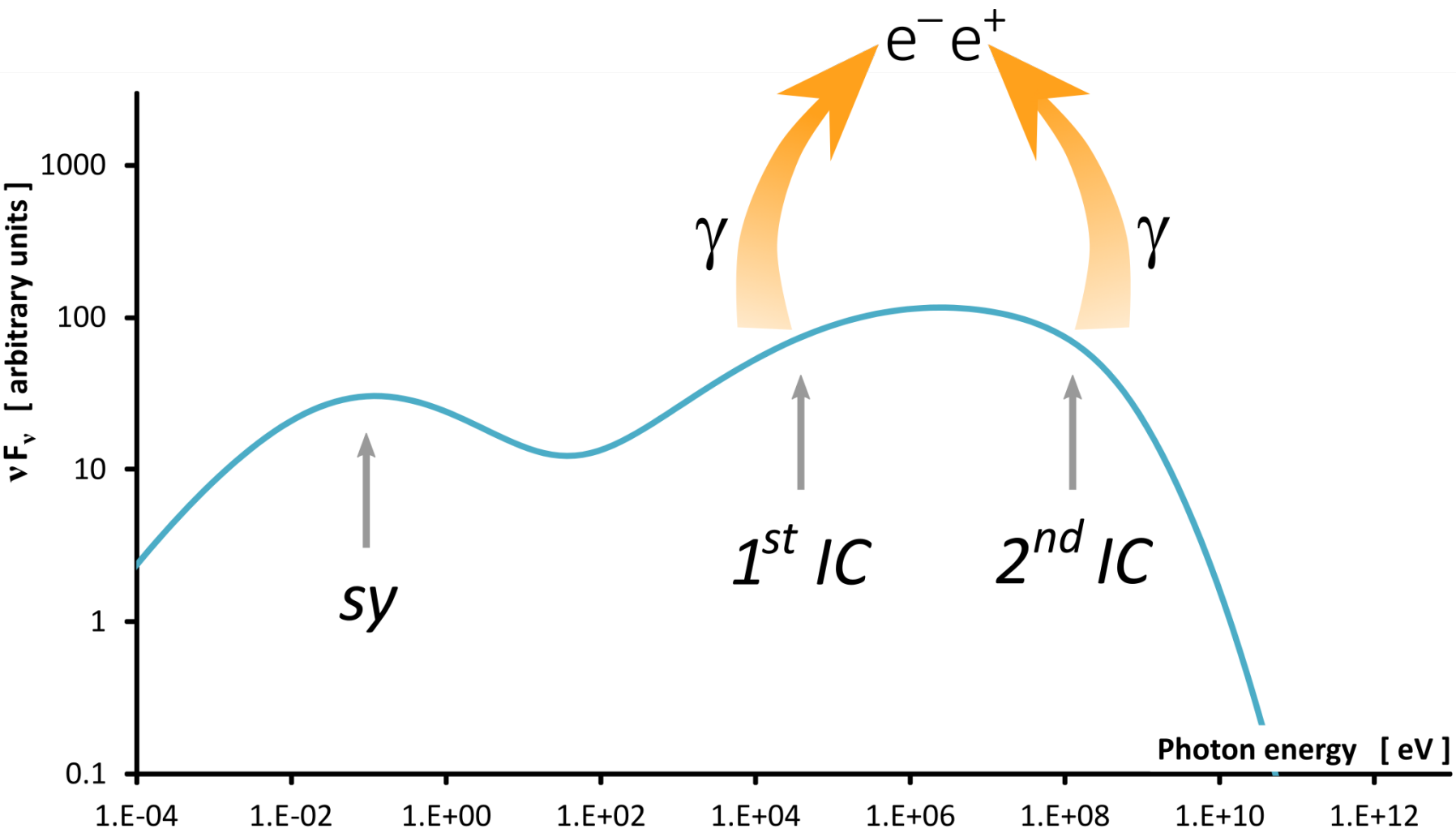
Balance condition — maximize fraction of absorbed radiation

1st order pair balance in a nutshell



Balance condition $\epsilon_{sy}\epsilon_{\rm IC} \sim m_e^2 c^4 \quad \Rightarrow \quad \langle \gamma_{inj} \rangle \sim (B/B_{cr})^{-1/3}$

2nd order pair balance



Balance condition $\epsilon_{\mathrm{IC},1}\,\epsilon_{\mathrm{IC},2} \sim m_e^2 c^4 \;\Rightarrow\; \langle \gamma_{inj} \rangle \sim (B/B_{cr})^{-1/5}$

Comparison of spectra for 1st and 2nd order solutions

	1st order	2nd order
synchrotron peak	~ 1 keV	~ 0.1 eV
location and width of IC peak	~ 0.1 TeV narrower than sy peak	~ 0.1 GeV wider than sy peak
IC to sy ratio	~ 1	$\gtrsim 1$ $(1 \div 100)$

Pair-balance model gives predictions

- Fraction of energy in accelerated electrons $\epsilon_e \sim 1$
- Luminosities in the highest-energy (efficiently absorbed) photons and in target (absorbing) photons are approximately equal
- Lorentz-factor of accelerated electrons $\langle \gamma_{\rm inj} \rangle$ is not a free parameter, but rather adjusted to satisfy either of the solutions

saturated (high compactness) solutions

- injection at $(B_{cr}/B)^{1/5} \lesssim \langle \gamma_{\rm inj} \rangle \lesssim (B_{cr}/B)^{1/3}$

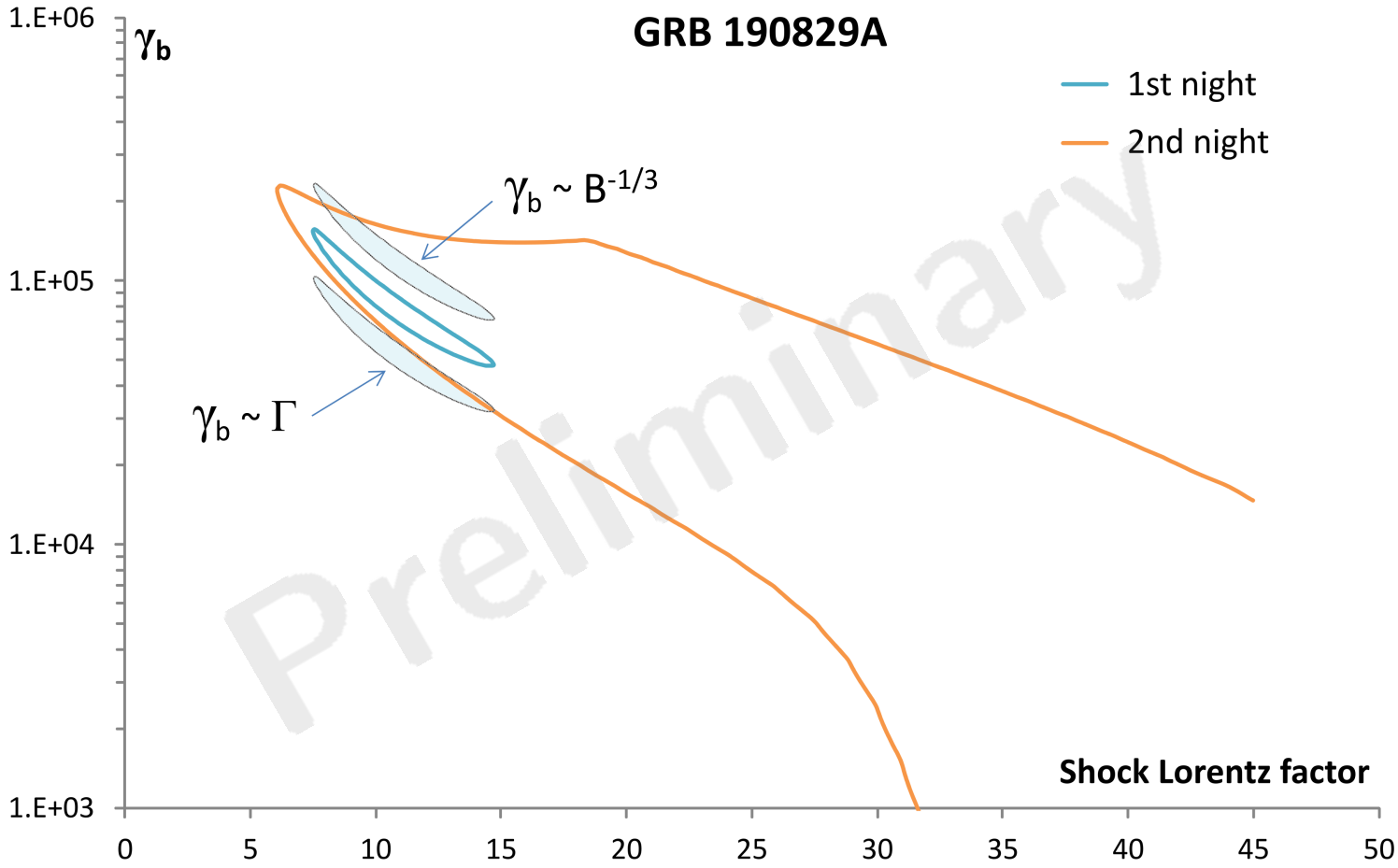
  keeps the fraction of internally absorbed radiation constant at ≈ 0.1

low compactness solutions

- injection at $\langle \gamma_{\rm inj} \rangle \sim (B_{cr}/B)^{1/3} \simeq 3.5 \times 10^4 \, (B/1\,{\rm G})^{-1/3}$

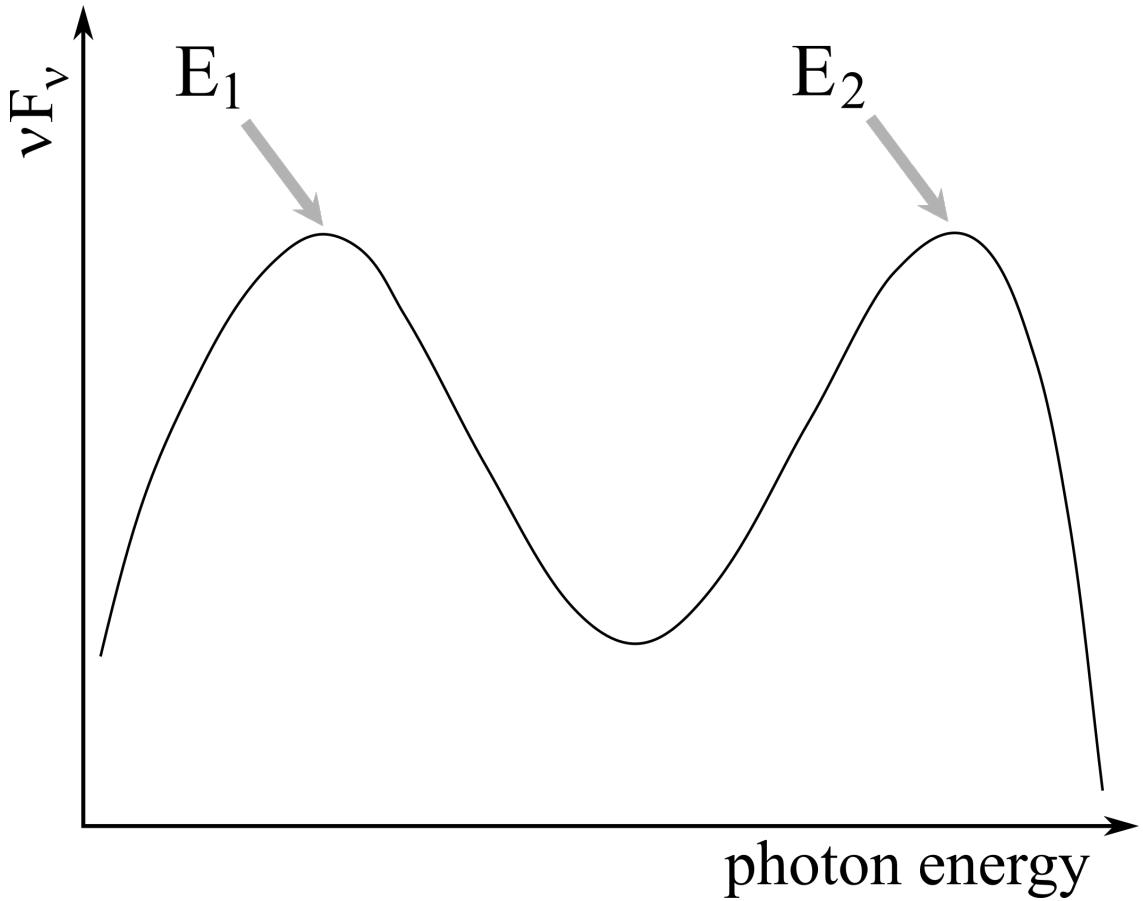
  maximizes the fraction of internally absorbed radiation

Evolution of the injection Lorentz factor



- there is an indication that injection Lorentz factor increases with time
- agrees with pair-balance prediction ($\langle\gamma_{\rm inj}\rangle \propto B^{-1/3}$ law)
- does not agree with conventional DSA assumption ($\langle\gamma_{\rm inj}\rangle \propto \Gamma_{sh}$ law)

Estimating parameters from spectrum shape within seconds

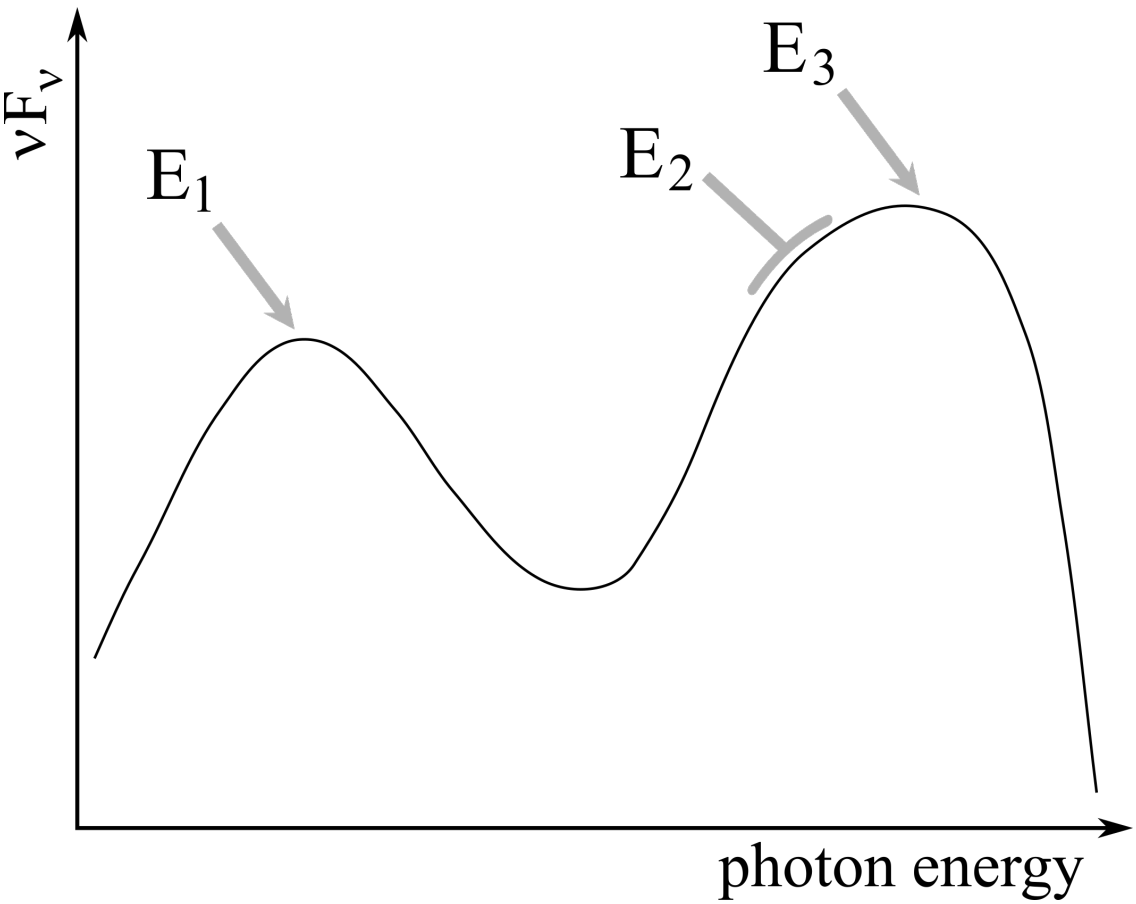


1. $\Gamma = \frac{\sqrt{E_1 E_2}}{m_e c^2}$

2. $\gamma_b = \sqrt{\frac{E_1}{E_2}}$

3. $\frac{B}{5 \cdot 10^{13}\ \mathrm{G}} = \left(\frac{E_1}{E_2}\right)^{\frac{3}{2}}$

Estimating parameters from spectrum shape within seconds



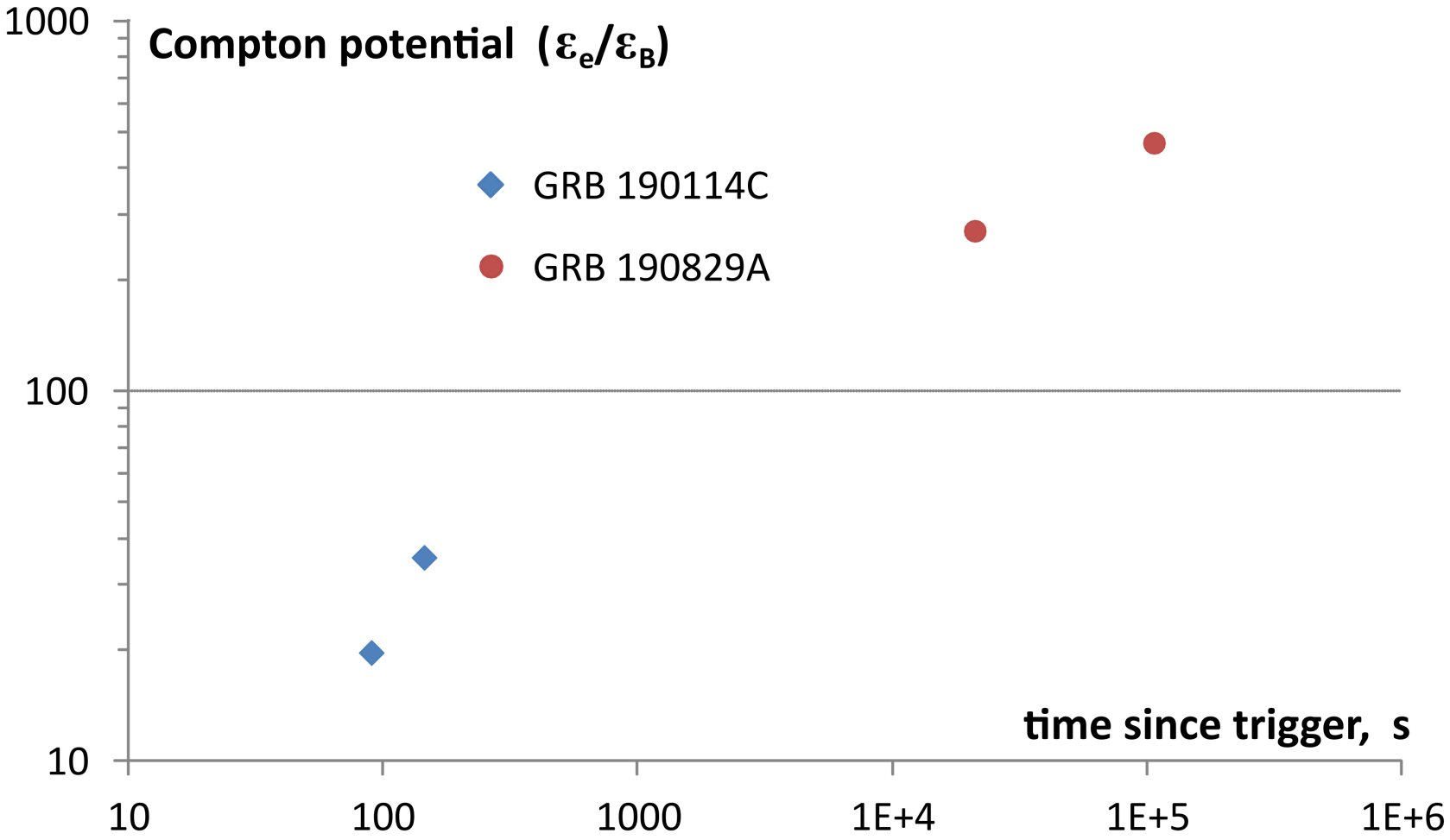
1. $\Gamma = \dfrac{\left(E_3^3 E_1\right)^{1/4}}{m_e c^2}$

2. $\gamma_b = \left(E_3/E_1\right)^{1/4}$

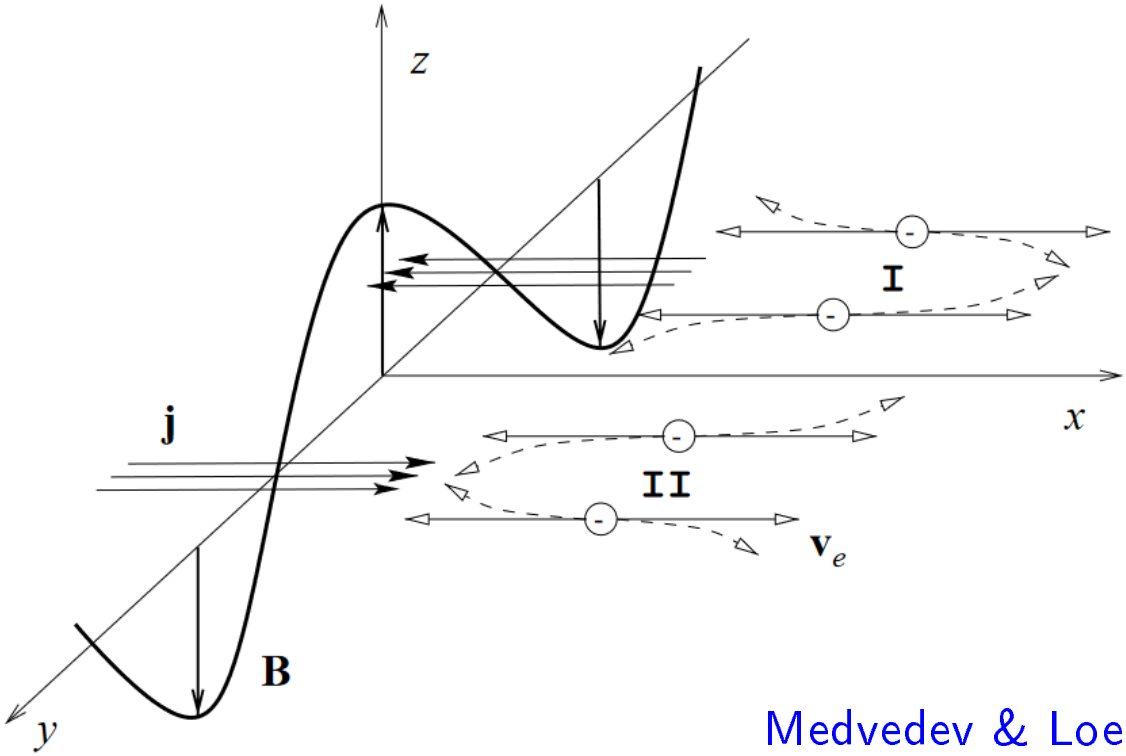
3. $\dfrac{B}{5\cdot 10^{13}\ \mathrm{G}} = \left(\dfrac{E_1}{E_2}\right)^{\frac{5}{4}}$

4. $k_{\mathrm{SC}} = \left(L_{\mathrm{IC}}/L_{\mathrm{sy}}\right)^2$

GRB afterglows: Compton potential changes with time



Magnetic field: Weibel instability



Medvedev & Loeb ApJ 526 (1999)

- forms a shock front in initially unmagnetized plasma
- allows generation of strong enough magnetic field
- even at saturation, the magnetic turbulence is linear: $r_g > \lambda_c$

Rise and decay of the magnetic field

Maximum increment $G_m \sim A^{3/2} \dfrac{\omega_p}{\gamma^{1/2}}$

corresponds to wavenumber $k_m \sim A^{1/2} \dfrac{\omega_p}{\gamma^{1/2} c}$

Decay at zero anisotropy $t'_{\rm dec} \simeq \dfrac{\omega_{\rm pl}^2 \lambda_c^3}{c^3} \quad (\lambda_c \equiv 1/k)$

$\Rightarrow$ decay time is of the order of rise time

Estimate for GRB afterglows

$$t_{dec} \sim t_{rise} \sim \frac{1}{\Gamma_{sh}} \left(\frac{\gamma_{pl}}{\omega_{pi}^2} \right)^{1/2} \sim 10^{-6} \mathrm{s} \left(\frac{300}{\Gamma_{sh}} \right) \left(\frac{10\ \mathrm{cm}^{-3}}{n} \right)^{1/2} \quad \text{for } A \sim 1$$

at early afterglow, i.e., $100 \div 1000$ seconds from trigger

Duration of synchrotron radiative cooling

Power of synchrotron radiation $\dot{E}_e = -\frac{4}{3}\gamma_e^2 \sigma_{\rm T} \frac{B^2}{8\pi} c$

Cooling time $t'_{cool} = \frac{6\pi m_e c}{\gamma_e \sigma_{\rm T} B^2}$ (comoving system)

Estimate for GRB afterglows

$$t_{cool} = \frac{1}{\Gamma_{sh}} \frac{6\pi m_e c}{\gamma_e \sigma_{\rm T} B^2} \simeq 30 \text{ s} \times \frac{300}{\Gamma_{sh}} \left(\frac{10^4}{\gamma_e}\right) \left(\frac{3 \text{ G}}{B}\right)^2$$

at early afterglow, i.e., $100 \div 1000$ seconds from trigger

The issue of short-lived magnetic field

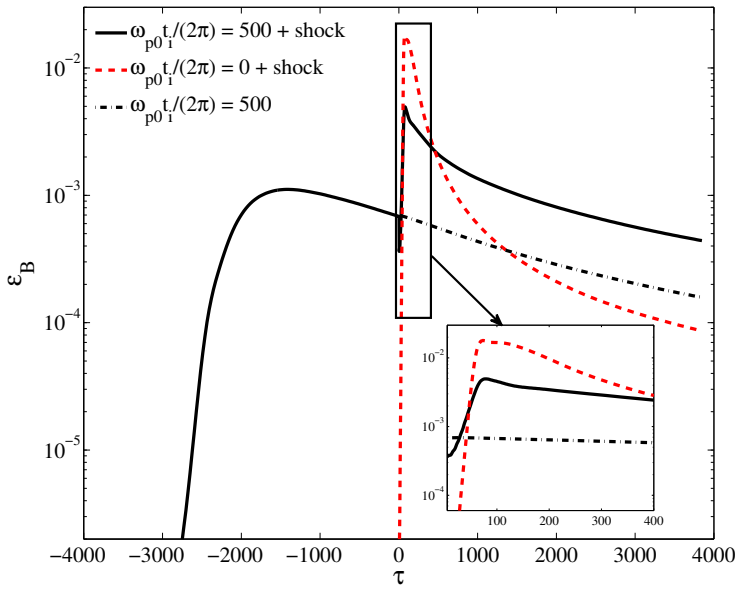
Synchrotron radiation efficiency $f_{sy} \lesssim \dfrac{t_{dec}}{t_{cool}}$

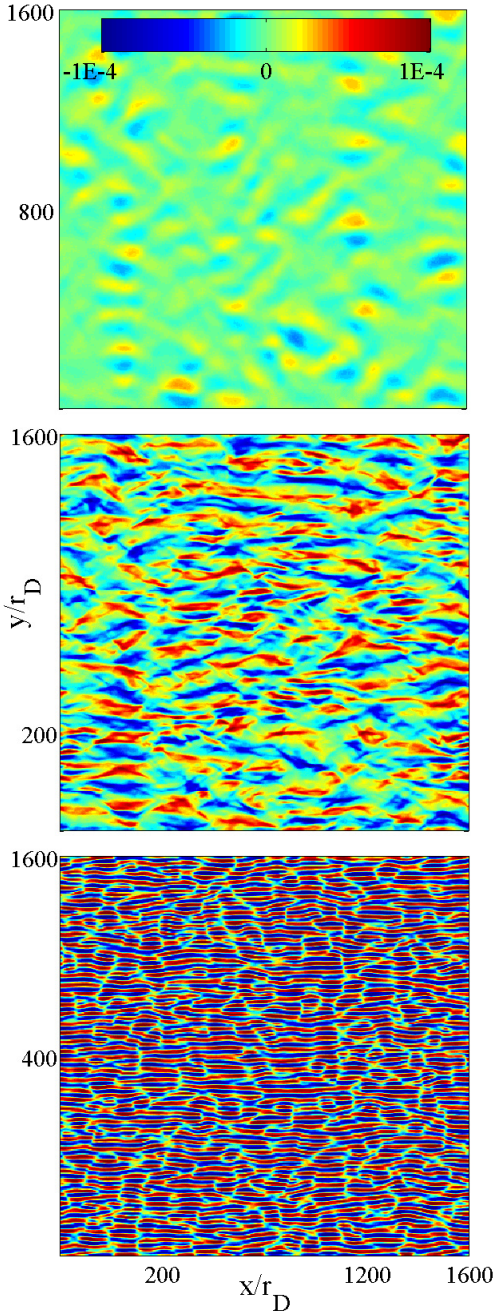
Observed afterglow brightness leads to estimate $f_{sy} > 0.01$

However

$$\frac{t_{dec}}{t_{cool}} = \left(\frac{\omega_{\rm pl}^2 \lambda_c^3}{c^3}\right)\left(\frac{\gamma_e \sigma_{\rm T} B^2}{6\pi m_e c}\right) \sim \boxed{10^{-5} \div 10^{-7}} \quad (\text{ if } \lambda_c \sim c/\omega_{pl})$$

Long injection causes long decay





No pre-injection

Magnetization evolution shown by red line.
Magnetic field distribution shortly after shock shown in bottom panel on the right.

With pre-injection

Magnetization evolution shown by solid black line.
Magnetic field distribution:
top panel on the right — just before shock
middle panel on the right — shortly after shock

From Garasev & ED, MNRAS 461 (2016)

Synchrotron radiation efficiency

$t_{dec} \ll t_{cool}$, fraction of comptonized radiation is not large

$$f_{sy} \lesssim \left(\frac{\lambda_c}{r_{\rm g,pl}}\right)^3 \left(\frac{\omega_{\rm pl}^2 r_{\rm g,pl}^3}{c^3}\right) \left(\frac{\gamma_e \sigma_{\rm T} B^2}{6\pi m_e c}\right)$$

- relate gyro-frequency to plasma frequency :

$$\omega_{\rm B} \simeq \frac{eB}{m_e c}, \qquad \omega_{\rm pl} \simeq \left(\frac{4\pi e^2 N c^2}{E_{\rm pl}}\right)^{1/2}$$

$$\Rightarrow \quad \frac{\omega_{\rm B}}{\omega_{\rm pl}} \simeq \frac{E_{\rm pl}}{m_e c^2}\left(\frac{B^2/4\pi}{N E_{\rm pl}}\right)^{1/2} = \sqrt{2\epsilon_{\rm B}}\,\frac{E_{\rm pl}}{m_e c^2}$$

$$f_{sy} \lesssim \left(\frac{\lambda_c}{r_{\rm g,pl}}\right)^3 \left(\frac{m_e c^2}{E_{\rm pl}}\right)^2 \left(\frac{\omega_{\rm B}^2 r_{\rm g,pl}^3}{2\epsilon_{\rm B} c^3}\right) \left(\frac{\gamma_e \sigma_{\rm T} B^2}{6\pi m_e c}\right)$$

Synchrotron radiation efficiency

$$f_{sy} \lesssim \left(\frac{\lambda_c}{r_{g,pl}}\right)^3 \left(\frac{m_e c^2}{E_{pl}}\right)^2 \left(\frac{\omega_B^2 r_{g,pl}^3}{2\epsilon_B c^3}\right) \left(\frac{\gamma_e \sigma_T B^2}{6\pi m_e c}\right)$$

- substitute magnetic field strength and Thomson cross-section :

$$B = \frac{m_e c}{e}\omega_B \quad \text{and} \quad \sigma_T = \frac{8\pi}{3}\left(\frac{e^2}{m_e c^2}\right)^2$$

$$f_{sy} \lesssim \left(\frac{\lambda_c}{r_{g,pl}}\right)^3 \left(\frac{m_e c^2}{E_{pl}}\right)^2 \left(\frac{\omega_B^2 r_{g,pl}^3}{2\epsilon_B c^3}\right) \left(\frac{4}{9}\frac{\gamma_e e^2 \omega_B^2}{m_e c^3}\right)$$

Synchrotron radiation efficiency

$$f_{sy} \lesssim \left(\frac{\lambda_c}{r_{\rm g,pl}}\right)^3 \frac{m_e c}{E_{\rm pl}^2} \left(\frac{\omega_{\rm B} r_{\rm g,pl}}{c}\right)^3 \left(\frac{2}{9}\frac{e^2 \gamma_e \omega_{\rm B}}{\epsilon_{\rm B}}\right)$$

- substitute energy of synchrotron photons and gyro-radius of plasma particles :

$$E_{\rm sy} \simeq \Gamma_{\rm sh} \gamma_e^2 \hbar \omega_{\rm B} \quad \Rightarrow \quad \gamma_e \omega_{\rm B} \simeq \frac{E_{\rm sy}}{\Gamma_{\rm sh} \hbar \gamma_e}$$

$$r_{\rm g,pl} = \frac{E_{\rm pl}}{m_e c^2} \frac{c}{\omega_{\rm B}}$$

$$f_{sy} \lesssim \left(\frac{\lambda_c}{r_{\rm g,pl}}\right)^3 \left(\frac{E_{\rm pl}}{\gamma_e m_e c^2}\right) \left(\frac{2}{9}\frac{e^2}{\hbar c}\frac{1}{\epsilon_{\rm B}}\frac{E_{\rm sy}/\Gamma_{\rm sh}}{m_e c^2}\right)$$

Synchrotron radiation efficiency

$$f_{sy} \lesssim \frac{2}{9}\frac{\alpha_f}{\epsilon_{\rm B}}\left(\frac{E_{\rm pl}}{\gamma_e m_e c^2}\right)\left(\frac{E_{\rm sy}/\Gamma_{\rm sh}}{m_e c^2}\right)\times\left(\frac{\lambda_c}{r_{\rm g,pl}}\right)^3$$

For typical parameters ($\epsilon_{\rm B}=0.004$, $E_{\rm sy}=5$ keV, $\Gamma=30$)

$$f_{sy} \lesssim 10^{-4}\left(\frac{E_{\rm pl}}{\gamma_e m_e c^2}\right)\times\left(\frac{\lambda_c}{r_{\rm g,pl}}\right)^3$$

Observations are only consistent with the case $r_{\rm g,pl} < \lambda_c$

- Magnetic turbulence in GRB afterglow shocks cannot be linear
- The acting magnetic field is MHD-driven

Can we still use one-zone radiation models?

Estimate whether the radiating electrons are captured in the magnetic field:

$$\frac{r_{\rm g,e}}{\lambda_c} = \frac{\gamma_e m_e c^2}{E_{\rm pl}} \frac{r_{\rm g,pl}}{\lambda_c} \quad \Rightarrow \quad \frac{r_{\rm g,e}}{\lambda_c} \lesssim \left(\frac{2}{9} \frac{\alpha_f}{\epsilon_{\rm B} f_{sy}} \frac{E_{\rm sy}/\Gamma_{\rm sh}}{m_e c^2} \right)^{1/3} \left(\frac{\gamma_e m_e c^2}{E_{\rm pl}} \right)^{2/3}$$

Estimate for $\epsilon_{\rm B} = 0.004$, $E_{\rm sy} = 5$ keV, $\Gamma = 30$, $f_{sy} = 0.1$:

$$\frac{r_{\rm g,e}}{\lambda_c} \lesssim 0.1 \left(\frac{\gamma_e m_e c^2}{E_{\rm pl}} \right)^{2/3}$$

Radiating electrons are *most likely* captured in the magnetic field

Can we still use one-zone radiation models?

Bohm diffusion

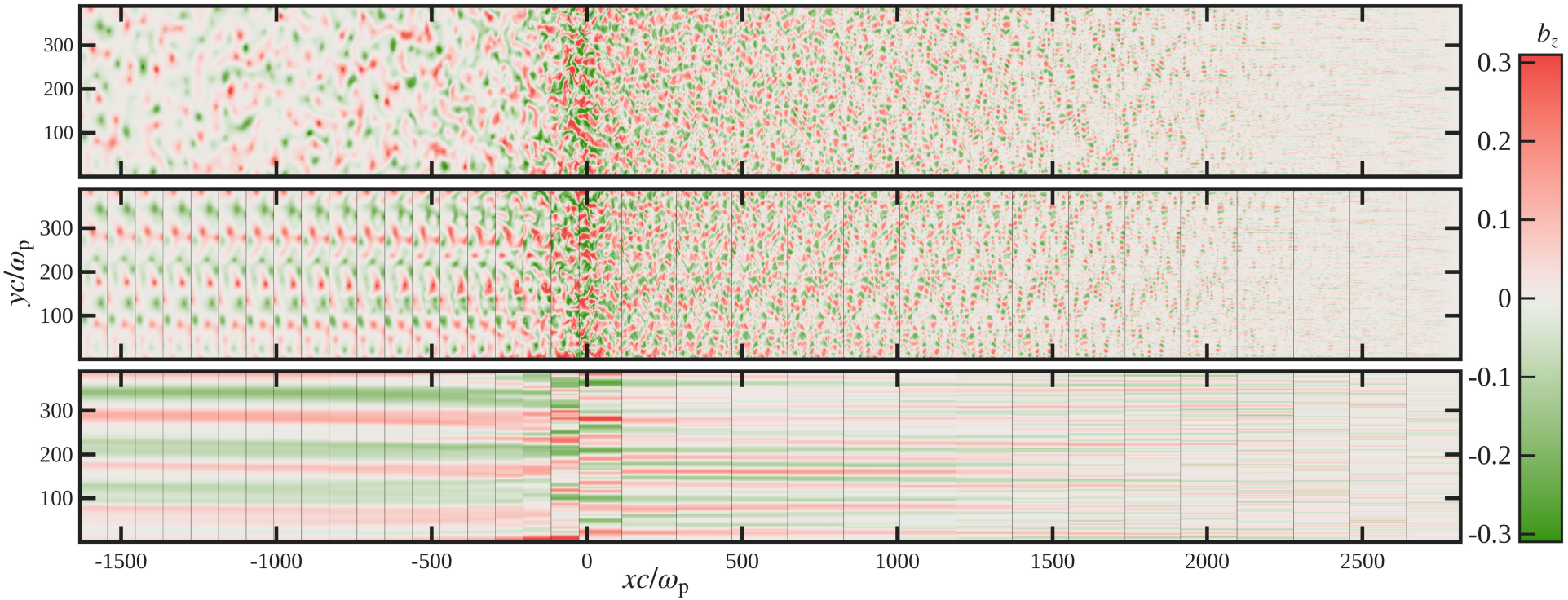
$$\ell_{\rm diff} \simeq \sqrt{D t_{\rm cool}} \simeq r_{\rm g,e}\sqrt{\omega_{\rm B}\, t_{\rm cool}/(3\gamma_e)} \quad \text{(diffusion coeff. } D = c r_{\rm g,e}/3\text{)}$$

$$\frac{\ell_{\rm diff}}{\lambda_c} \lesssim \left(\frac{1}{48}\,\frac{1}{\epsilon_{\rm B}^2 f_{\rm sy}^2}\,\frac{\Gamma_{\rm sh}\; m_e c^2}{\alpha_f E_{\rm sy}}\right)^{1/6}\left(\frac{\gamma_e m_e c^2}{E_{\rm pl}}\right)^{2/3} \sim 60\left(\frac{\gamma_e m_e c^2}{E_{\rm pl}}\right)^{2/3}$$

(for the estimate we take $\epsilon_{\rm B} = 0.004$, $E_{\rm sy} = 5$ keV, $\Gamma = 30$, $f_{\rm sy} = 0.1$)

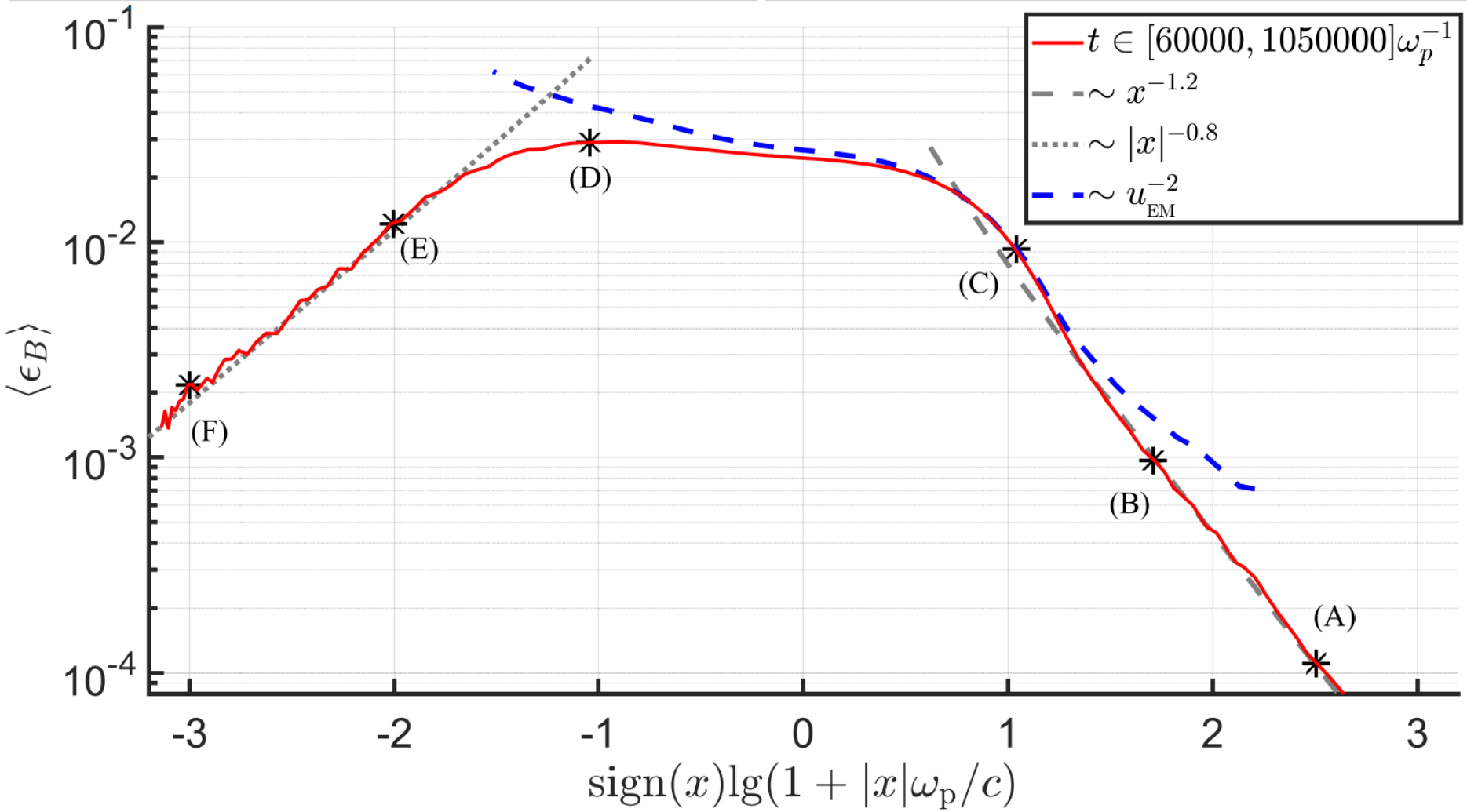
- diffusion ensures efficient sampling and hence averaging of the entire distribution of local magnetic field strengths
- one-zone approximation is still valid

Magnetic field map across the simulation box



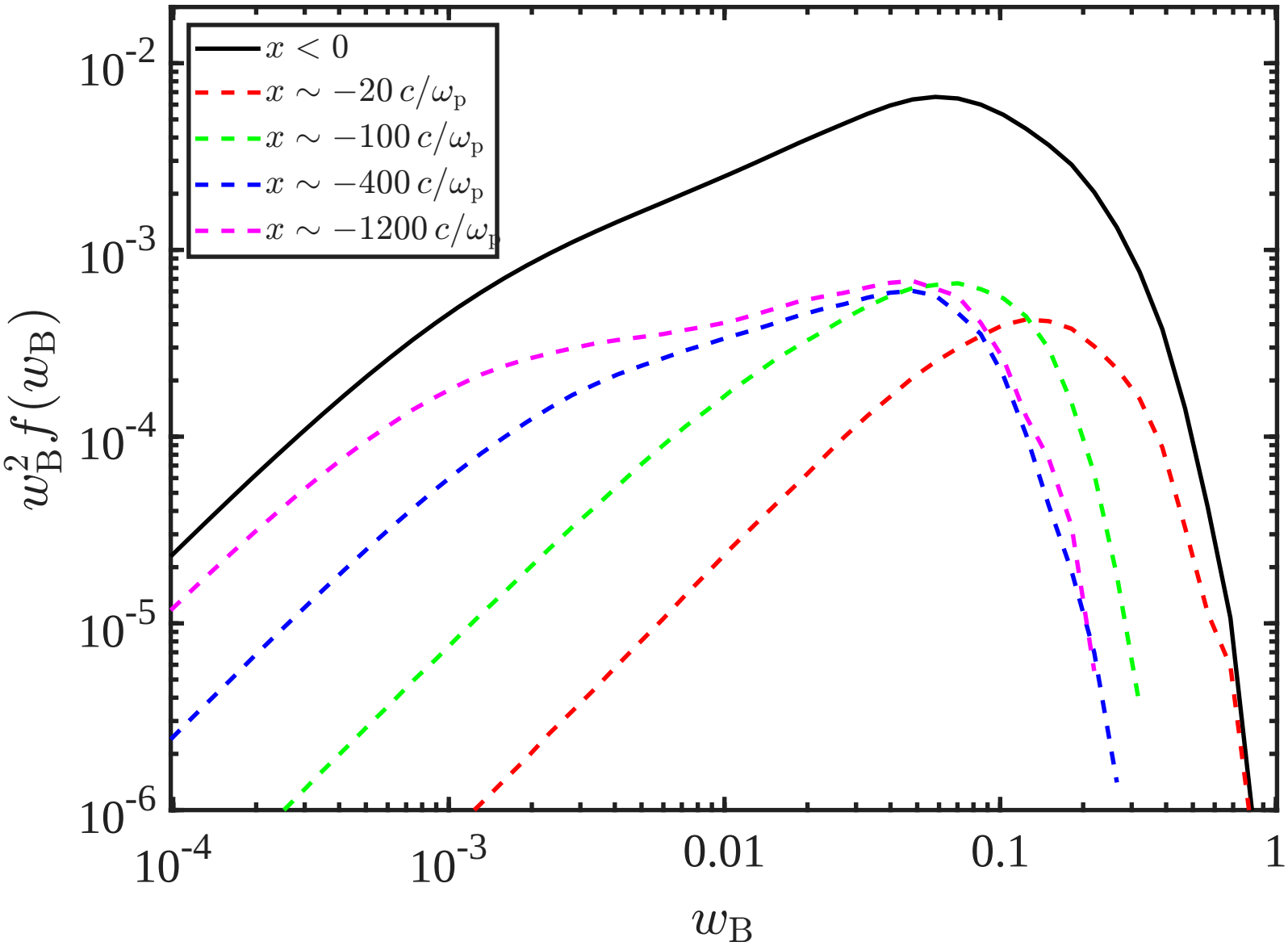
Garasev & ED, to appear on arXiv

Evolution of magnetization along the flow



Garasev & ED, to appear on arXiv

Skewed magnetic energy density distribution



Garasev & ED, to appear on arXiv

Far-reaching insights from the very recent PIC simulations

... **if** *the magnetic field evolves in the same manner further downstream*
... **if** *we can extend the results from 2D to 3D*

- Intergal of the synchrotron-emission power diverges downstream
  $\Rightarrow$ every electron finds a place to radiate all its energy
- The synchrotron power is set by $\epsilon_{\rm B}$, but the peak frequency is set by ϵ_e
- Transition in single-particle synchrotron spectrum asymptotics:
  $F_\nu \propto \nu^{1/3} \longrightarrow F_\nu = \text{const}$

Summary 2

- Conventional diffusive shock acceleration is inefficient in relativistic shocks
- There is good evidence that actually working acceleration mechanism in GRB afterglow shocks is converter
- Pair-balance model is interplay of converter acceleration and synchrotron + IC radiation.
  Allows quick characterization of emitting zones from sketchy obs. data
- Magnetic field generation and decay is the least understood part of the problem. Recent advances in theory and PIC simulations point to persistent isolated magnetic structures as a solution to the issue of short-lived magnetic field